Product Branching Ratios of the HCO + NO_2 Reaction

Kwang Taeg Rim and John F. Hershberger*

Department of Chemistry, North Dakota State University, Fargo, North Dakota 58105

Received: February 26, 1998; In Final Form: April 21, 1998

The reaction of HCO radicals with NO_2 was studied at 298 K using time-resolved infrared diode laser spectroscopy to detect CO, CO_2, and NO products. HCO was formed by the reaction of photolytically produced chlorine atoms with H_2CO. After quantifying product yields and considering likely secondary reactions, we obtain the following product branching ratios: CO + NO + OH accounts for 63 ± 5%, and H + NO + CO_2 accounts for the remaining 37 ± 5%. Upper limits of 10% are estimated for the CO + HONO and HNO + CO_2 channels.

Introduction

The formyl radical HCO is an important intermediate in combustion chemistry and atmospheric chemistry. The reaction of HCO with NO_2 is of interest in modeling nitrogen oxide pollutant formation and removal,[1] as well as models of the oxidation of formaldehyde. Several product channels are possible:

$$HCO + NO_2 \rightarrow CO + NO + OH \qquad \Delta H^0_{298} = -57.86 \text{ kJ/mol} \quad (1a)$$

$$\rightarrow H + NO + CO_2 \qquad \Delta H^0_{298} = -161.85 \text{ kJ/mol} \quad (1b)$$

$$\rightarrow HONO + CO \qquad \Delta H^0_{298} = -265.97 \text{ kJ/mol} \quad (1c)$$

$$\rightarrow HNO + CO_2 \qquad \Delta H^0_{298} = -370.56 \text{ kJ/mol} \quad (1d)$$

where thermochemical data were obtained from JANAF thermochemical tables.[2]

Several previous measurements of the total rate constant and branching ratios of this reaction have been reported. Morrison and Heicklen estimated $k_1 = (2.7 \pm 0.9) \times 10^{-11}$ cm^3 molecule^{-1} s^{-1} at 296 K by a relative rate technique and suggested that channel 1b is the major product channel.[3,4] In more direct experiments, Timonen et al. used 308 nm photolysis of CH_3CHO combined with photoionization mass spectrometry to detect HCO and obtained an Arrhenius expression for the total rate constant $k_1 = (2.5 \times 10^{-11}) \exp[+216.5/T]$ cm^3 molecule^{-1} s^{-1} over the range 294−713 K.[5] He et al.[6] investigated the thermal reaction of CH_2O with NO_2 using FTIR product analysis and performed kinetic modeling of product concentration−time curves to fit a moderately complex reaction mechanism. They attributed product formation due to channels 1b and 1c and estimated $k_{1c} = 2.82 \times 10^{-11}$ cm^3 molecule^{-1} s^{-1} and $k_{1b} = 1.48 \times 10^{-11}$ cm^3 molecule^{-1} s^{-1} over the range 393−476 K, i.e., branching ratios of $\phi_{1c} = 0.66$ and $\phi_{1b} = 0.34$.[6] Recently, Guo et al. studied the reaction at room temperature using 308 nm photolysis of CH_3CHO and detecting HCO by visible laser absorption and CO_2 and HONO by difference-frequency near-infrared absorption spectroscopy. They obtain $k_1 = (5.7 \pm 0.9) \times 10^{-11}$ cm^3 molecule^{-1} s^{-1} at 296 K, and $\phi_{1b} + \phi_{1d} = 0.52 \pm 0.14$ based on the observed CO_2 yield.[7] They were unable to detect HNO and therefore suggested that most of the CO_2 originates from channel 1b and that channel 1c accounts for the remaining 48% of the reaction. BAC-MP4 ab initio calculations have been used to estimate the energies of $HC(O)NO_2$ and HC(O)ONO complexes at 208.4 and 251.0 kJ below the reactants.[8] No higher level calculations of transition-state structures or energetics have been reported.

One of the major difficulties in product branching ratio measurements is contribution of secondary reactions to the observed product yields. For example, the photolysis of CH_3CHO produces HCO + CH_3, CH_4 + CO, and H + CH_3CO products. Reactions such as CH_3 + NO_2, H + NO_2, CH_3CO + NO_2, etc., substantially complicate the interpretation of product yields. Photolysis of H_2CO in its well-known 270−360 nm absorption band produces H + HCO and H_2 + CO, leading to similar problems. The approach used in this study is to form HCO by the abstraction reaction

$$Cl + H_2CO \rightarrow HCl + HCO \qquad (2)$$

This reaction is fast, with $k_2 = 7.32 \times 10^{-11}$ cm^3 molecule^{-1} s^{-1}.[9] In this way, HCO is formed without concurrent formation of H atoms or other radical species. We have attempted both S_2Cl_2 and $^{15}N^{18}OCl$ as chlorine atom precursors and found that $^{15}N^{18}OCl$ is the preferred precursor because it is relatively free of secondary chemistry. This molecule has a significant absorption coefficient and Cl atom quantum yield at 248 nm, while the absorption coefficients of H_2CO and NO_2 at this wavelength are quite small. $^{15}N^{18}O$ formed during the photolysis of $^{15}N^{18}OCl$ is spectroscopically distinguishable from unlabeled NO formed by the title reaction. Note that the reaction of Cl with NO_2 is termolecular[10] and therefore very slow at the total pressures (1−2 Torr) used in this study. We then use time-resolved infrared diode laser absorption spectroscopy to quantify yields of NO, CO, and CO_2 products produced by photolysis of $^{15}N^{18}OCl/CH_2O/NO_2$/buffer gas mixtures.

Experimental Section

The experimental procedure is similar to that described in previous publications.[11−13] A diagram of the apparatus is shown

S1089-5639(98)01311-5 CCC: $15.00
Published on Web 06/18/1998

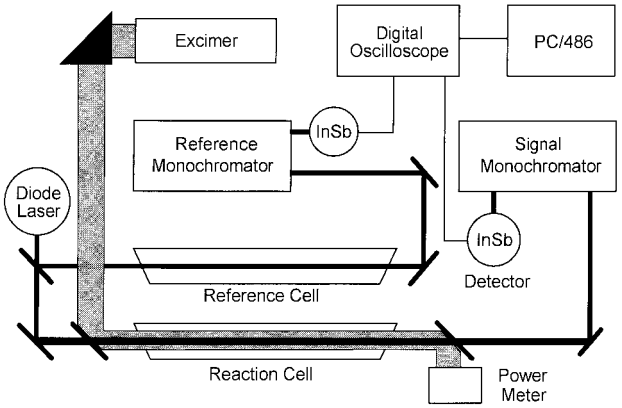

Figure 1. Diagram of the experimental apparatus.

in Figure 1. Briefly, 248 nm photolysis light was provided by an excimer laser (Lambda Physik Compex 200). Several lead salt diode lasers (Laser Photonics) operating in the 80−110 K temperature range were used to provide tunable infrared probe laser light. The IR beam was collimated by a lens and combined with the UV beam using a dichroic mirror, and both beams were copropagated through a 1.46 m absorption cell. After removal of the UV light by means of a second dichroic mirror, the infrared beam was then passed into a $^1/_4$ m monochromator and focused onto a 1 mm InSb detector (Cinncinati Electronics, ∼1 μs response time). Transient infrared absorption signals were recorded on a LeCroy 9310A digital oscilloscope and transferred to a computer for analysis.

SF_6, CF_4, and NO_2 (Matheson) were purified by repeated freeze−pump−thaw cycles at 77 K. NO_2 was further purified by freeze−pump−thaw cycles at 220 K to remove NO impurities. CH_2O was formed by heating paraformaldehyde (Aldrich) under vacuum. $^{15}N^{18}OCl$ was synthesized[14] by bubbling isotopically labeled $^{15}N^{18}O$ (Isotec) through liquid Cl_2 (Matheson) at 200 K and purified by freeze−pump−thaw cycles at 200 K.

CO, CO_2, and NO (unlabeled) product molecules were probed in this experiment using the following spectral lines:

$$NO(v=0,J=7.5) \rightarrow NO(v=1,J=8.5),$$
$$R(7.5) \text{ line at } 1903.123 \text{ cm}^{-1}$$

$$CO(v=0,J=16) \rightarrow CO(v=1,J=15),$$
$$P(16) \text{ line at } 2077.650 \text{ cm}^{-1}$$

$$CO_2((00^00),J=2) \rightarrow CO_2((00^01),J=1),$$
$$P(2) \text{ line at } 2347.576 \text{ cm}^{-1}$$

The HITRAN molecular database was used as an aid in the location and assignment of spectral lines.[15] Typical reaction conditions were 0.1 Torr of NOCl, 0.1 Torr of CH_2O, 0.05−0.2 Torr of NO_2, and 1.0 Torr of SF_6 or CF_4 buffer gas.

Results

Typical time-resolved transient absorption signals upon photolysis of a $^{15}N^{18}OCl/CH_2O/NO_2/CF_4$ mixture are shown in Figure 2. Resonant absorption signals were obtained by tuning the diode laser to the center of the spectral line of a product molecule probed. The off-resonant signals were also collected with the diode laser detuned ∼0.02 cm^{-1} off of the spectral line. These off-resonance signals are an artifact due to thermal deflection of the infrared laser beam upon transient heating of the gas mixture by the photolysis excimer laser. The transient absorption signal shown in the top trace of Figure 2 was obtained

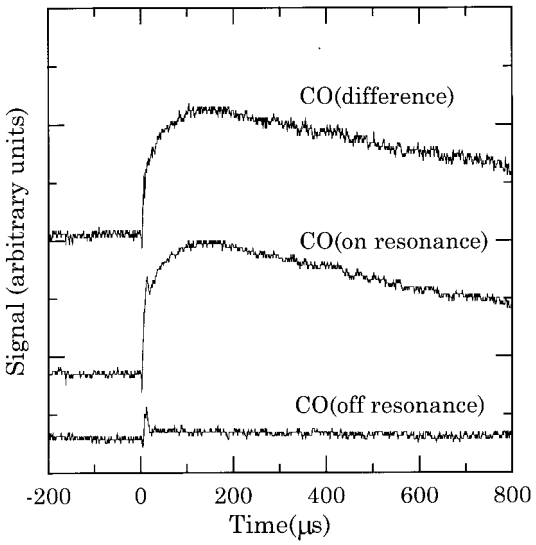

Figure 2. Transient signals for CO (P(16) line at 2077.650 cm^{-1}). Bottom trace: off-resonant (detuned ∼0.02 cm^{-1}) signal. Middle trace: on-resonance signal. Top trace: difference of on-resonance and off-resonance signals. Reaction conditions: P_{NOCl} = 0.1 Torr, P_{H_2CO} = 0.1 Torr, P_{NO_2} = 0.2 Torr, P_{CF_4} = 1.0 Torr.

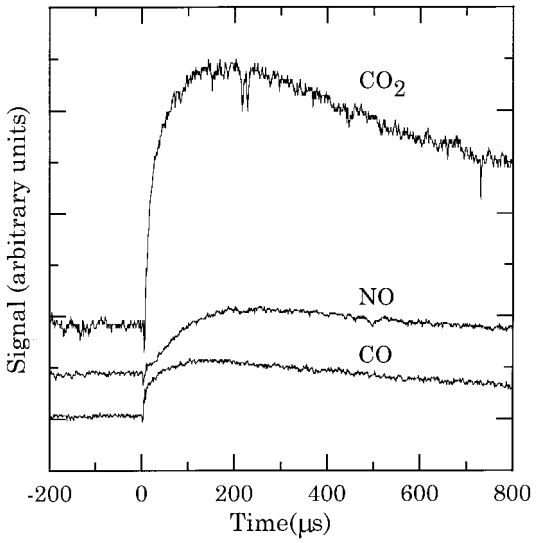

Figure 3. Transient signals for NO, CO, and CO_2 molecules. Reaction conditions: P_{NOCl} = 0.1 Torr, P_{H_2CO} = 0.1 Torr, P_{NO_2} = 0.2 Torr, P_{SF_6} = 1.0 Torr (for CO_2, NO), P_{CF_4} = 1.0 Torr (for CO).

by subtracting the off-resonant signals from the on-resonant signals. Figure 3 shows typical transient signals after this background subtraction for all of the molecules probed.

Given the fast rate constant of the title reaction, one expects the reaction to occur on a time scale of a few microseconds at our experimental conditions of 0.05−0.2 Torr of NO_2. The much slower rise time of about 200 μs observed in the transient absorption signals is attributed to the fact that products are produced in a large number of vibrational and rotational quantum states and that vibrational relaxation into the probed ground state is significantly slower than the reaction rate. Previous work[11−13] has shown that SF_6 is a suitable buffer gas for relaxing CO_2 and NO molecules but is extremely inefficient at relaxing vibrationally excited CO. CF_4 buffer gas is a more efficient vibrational relaxer of CO and was therefore used when probing these molecules.

Absorption signals at peak amplitude were converted to number densities using tabulated line strengths[15] and equations

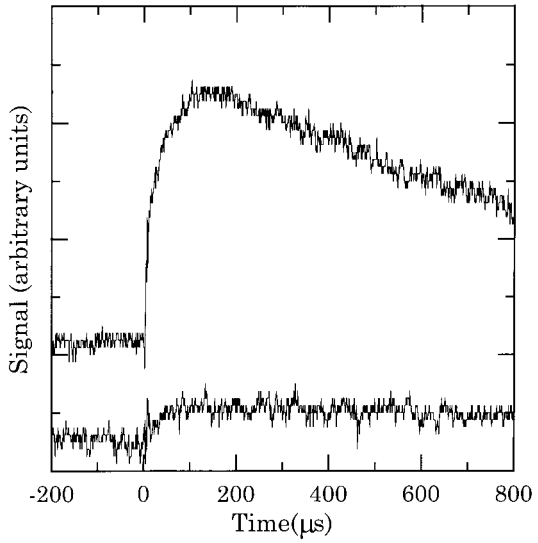

Figure 4. Comparison of transient signals for CO collected with and without precursor molecules. Top trace: $P_{NOCl} = 0.1$ Torr. Bottom trace: $P_{NOCl} = 0.0$ Torr. Both traces: $P_{NO_2} = 0.2$ Torr, $P_{CH_2O} = 0.1$ Torr, $P_{SF_6} = 1.0$ Torr.

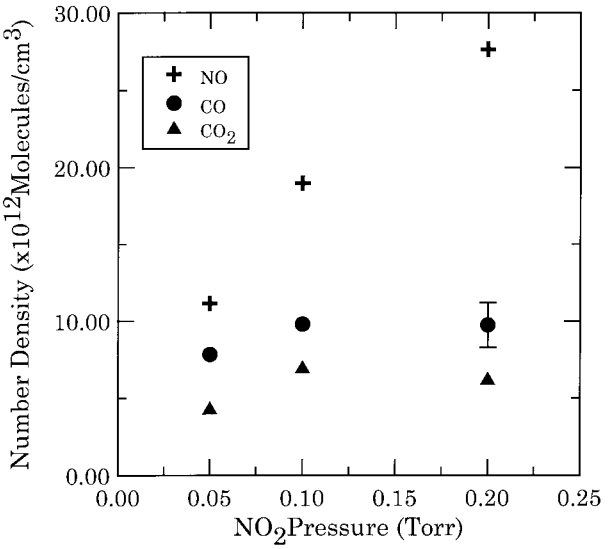

Figure 5. Product yields of CO, NO, and CO_2 as a function of NO_2 pressure. Reaction conditions: $P_{NOCl} = 0.1$ Torr, P_{NO_2} = variable, $P_{CH_2O} = 0.1$ Torr, $P_{SF_6} = 1.0$ Torr (for CO_2, NO), $P_{CF_4} = 1.0$ Torr (for CO).

described in earlier publications.[11−13] The line strengths of spectral lines probed for CO_2, CO, and NO are $S_{vj} = 6.87 \times 10^{-19}$, 1.18×10^{-19}, and 6.04×10^{-20} cm/molecule, respectively. Some absorption signals were also analyzed by fitting the decaying portion of each transient to an exponential function and extrapolating to $t = 0$. This approach gives amplitudes 18−22% larger than the peak amplitudes for each molecule detected. As is discussed below, our branching ratio determination is based on ratios of product yields and not absolute concentrations. Since the extrapolation was very nearly the same for each molecule, the ratios of product yields were unaffected by this analysis.

Several minor secondary reactions can occur in the absence of the NOCl photolysis precursor. For example, NO_2 has a small but nonnegligible absorption coefficient at 248 nm, resulting in the formation of NO.[16] CH_2O also absorbs weakly at 248 nm, forming H_2 + CO and H + HCO.[10] All of the detected products can then be formed by the title reaction using HCO formed in this way. Figure 4 shows a comparison of transient signals with and without NOCl precursor. Since these background signals were small, it was deemed appropriate to subtract the product yields obtained in the absence of NOCl from those obtained with the full reaction mixture. This was generally a small correction of ∼10−15% at 0.1 Torr of NO_2 but was somewhat larger at higher NO_2 pressures. After making these corrections, the product yields of CO, CO_2, and NO as a function of NO_2 pressure are shown in Figure 5.

Several other control experiments were performed to check for contributions from other secondary processes. For example, no $^{14}N^{16}O$ was detected upon photolysis of a $^{15}N^{18}OCl/SF_6$ mixture, indicating that the isotopic purity of the nitrosyl chloride sample was good. Upon photolysis of a $^{15}N^{18}OCl/NO_2/SF_6$ mixture, a small $^{14}N^{16}O$ signal with a very slow ∼1 ms rise time was observed. This is attributed to products of the termolecular Cl + NO_2 reaction, which is expected to be slow under the conditions used. Since this reaction is suppressed by reaction 2 when H_2CO is included in the reaction mixture, this is not expected to significantly affect the results.

In addition to CO, NO, and CO_2 products, we attempted to detect HNCO and HCNO products in this reaction, using tabulated line positions.[17,18] Formation of HNCO + O_2 as an additional product channel is thermodynamically possible, while HCNO + O_2 formation is significantly endothermic. Neither of these channels is mechanistically likely, however, and we observed no transient signals for either HNCO or HCNO. Line strengths for these molecules are not available, so we are unable to estimate a reliable upper limit, but it is clear that the yield of these channels is extremely small.

Discussion

Several features of the product yield curves shown in Figure 5 are notable. The CO and CO_2 yields are nearly independent of NO_2 pressure, suggesting that nearly all of the HCO radicals formed in reaction 2 react with NO_2 to form products. The NO yield, which is the largest of the three, is somewhat more dependent on NO_2 pressure, however. At the lowest NO_2 pressure used of 0.05 Torr, the NO yield is approximately equal to the sum of the CO and CO_2 yields. At the higher NO_2 pressures, however, the NO yield is approximately equal to [CO] + 2[CO_2]. This effect is attributed to the fast secondary reaction of hydrogen atoms with NO_2:

$$H + NO_2 \rightarrow NO + OH \qquad (3)$$

where $k_3 = 1.4 \times 10^{-10}$ cm^3 molecule^{-1} s^{-1}.[19] If channels 1a and 1b dominate in this reaction, then one NO molecule is formed for each CO molecule produced in channel 1a. One NO molecule is directly formed for each CO_2 molecule in channel 1b, but the concurrently produced hydrogen atom results in production of additional NO via reaction 3. In the limit of high NO_2 pressure, one expects every H atom formed to react with NO_2, resulting in a predicted total NO yield of $[NO]_{total} = [CO] + 2[CO_2]$. The experimental NO yield obtained at 0.2 Torr of NO_2 is within 10−15% of this prediction. At lower NO_2 pressures, other reactions, such as H + $^{15}N^{18}OCl \rightarrow$ HCl + $^{15}N^{18}O$, compete for hydrogen atoms, resulting in a lower yield of the unlabeled NO.

Suppose however that most of the CO is formed not by channel 1a but instead by channel 1c. Unless subsequent secondary reactions involving HONO result in NO formation, we predict [NO] = 2[CO_2] (if all H atoms react with NO_2). This is much lower than the experimentally observed NO yield.

The most likely secondary reaction involving HONO would be with NO_2:

$$HONO + NO_2 \rightarrow HNO_3 + NO \quad (4)$$

Using detailed balance and a measurement of the rate of the reverse reaction, Streit et al. report a very small upper limit for the rate constant of this reaction of $k_4 < 10^{-22}$ cm^3 molecule^{-1} s^{-1}.[20] It appears therefore that this reaction does not occur on the time scale of our experiment. The observed NO yields are therefore evidence that channel 1a predominates over channel 1c.

A similar argument can be made for channels 1b and 1d. If CO_2 is formed primarily by channel 1d rather than channel 1b, the predicted NO yield is also too small unless the following reaction occurs:

$$HNO + NO_2 \rightarrow NO + HONO \quad (5)$$

Unfortunately, no direct experimental data currently exist for this reaction, but a very small value of $k_5 = 3.5 \times 10^{-14}$ cm^3 molecule^{-1} s^{-1} at 298 K has been recommended.[19] If this value is reliable, reaction 5 takes place on a ~10 ms time scale under our conditions and therefore has negligible effect on the transient signal time scale of ~200 μs.

Several other potential secondary reactions deserve brief mention. Radical−radical reactions such as H + HCO, OH + HCO, HCO + HCO, etc., have large rate constants[21] but are probably negligible because the radical densities are about a factor of 100 lower than that of NO_2, so that any HCO formed is expected to react predominately with NO_2 and not other radicals. The Cl + NO_2 and OH + NO_2 reactions are termolecular[10,19,22] and are expected to be rather slow at the low total pressures used in these experiments. The OH + OH → H_2O + O reaction is also fairly slow with a rate constant of (1.4−1.9) × 10^{-12} cm^3 molecule^{-1} s^{-1},[22] and combined with the low radical densities present it is not expected to be significant on the experimental time scale. Some reactions that do occur are

$$Cl + {}^{15}N^{18}OCl \rightarrow {}^{15}N^{18}O + Cl_2 \quad (6)$$

$$H + {}^{15}N^{18}OCl \rightarrow {}^{15}N^{18}O + HCl \quad (7)$$

where $k_6 = 8.1 \times 10^{-11}$ and $k_7 = 1.8 \times 10^{-11}$ cm^3 molecule^{-1} s^{-1} at 298 K.[10,23] Although reaction 6 competes with reaction 2 for chlorine atoms and reaction 7 competes with reaction 3 for H atoms, any $^{15}N^{18}O$ formed in these reactions is spectroscopically distinguishable from the detected unlabeled NO. The HCO + Cl_2 reaction is quite slow, with $k = 5.6 \times 10^{-12}$ cm^3 molecule^{-1} s^{-1} at 298 K,[4] and does not compete effectively with the title reaction for formyl radicals.

On the basis of the above analysis, we conclude that channels 1a and 1b predominate. The branching ratio into these two channels can then be obtained from the observed CO and CO_2 yields: ϕ_{1a} = [CO]/([CO] + [CO_2]) and ϕ_{1b} = [CO_2]/([CO] + [CO_2]). Branching ratios calculated in this manner were independent of the NO_2 pressure used. We obtain $\phi_{1a} = 0.63 \pm 0.05$ and $\phi_{1b} = 0.37 \pm 0.05$, where the uncertainties represent one standard deviation. Our results are shown along with other literature values in Table 1. On the basis of the estimated precision of the NO yield measurements, we estimate upper limits of roughly 0.10 on the contribution of channels ϕ_{1c} and ϕ_{1d}.

TABLE 1: Product Branching Ratios of the HCO + NO_2 Reaction

product channel	this work	ref 7	ref 6
CO + NO + OH	0.63 ± 0.05		
H + NO + CO_2	0.37 ± 0.05	0.52 ± 0.14	0.34
HONO + CO	<0.10	0.48 ± 0.14	0.66
HNO + CO_2	<0.10	<0.10	

TABLE 2: Reactions Used in Kinetic Modeling Simulations

reaction	k (298 K), cm^3 molecule^{-1} s^{-1}	ref
Cl + H_2CO → HCl + HCO	7.9 × 10^{-11}	9
HCO + HCO → H_2CO + CO	5.0 × 10^{-11}	21
HCO + NO_2 → CO + HO + NO	3.6 × 10^{-11}	7, this work
HCO + NO_2 → CO_2 + H + NO	2.1 × 10^{-11}	7, this work
H + NO_2 → OH + NO	1.4 × 10^{-10}	19
Cl + $^{15}N^{18}OCl$ → $^{15}N^{18}O$ + Cl	8.1 × 10^{-11}	10
OH + H_2CO → H_2O + HCO	1.0 × 10^{-11}	21
H + $^{15}N^{18}OCl$ → HCl + $^{15}N^{18}O$	1.8 × 10^{-11}	23
H + HCO → H_2 + CO	1.5 × 10^{-10}	21
OH + HCO → H_2CO + CO	1.7 × 10^{-10}	21

An additional potential complication is the OH + CH_2O → HCO + H_2O reaction, which is rather fast, with $k = 1.0 \times 10^{-11}$ cm^3 molecule^{-1} s^{-1}.[23] OH radicals formed in reactions 1a and 3 can therefore re-form HCO reactants, leading to a slow chain mechanism which will increase the total product yield over that expected from the photolytically produced radical concentration. This process is probably occurring to some extent, although it competes with other OH removal routes such as OH + $^{15}N^{18}OCl$, diffusion, and the OH reactions mentioned above. It is difficult for us to estimate how much of our products originate from this effect because we do not know the photolysis quantum yield for Cl atom production from NOCl and are therefore unable to obtain a reliable estimate of the initial number of formyl radicals produced in reaction 2. Our branching ratio measurement, however, is not dependent on knowledge of $[HCO]_0$ because we probe all channels and obtain ϕ_{1a} and ϕ_{1b} from the [CO]/[CO_2] ratios, not the absolute product concentrations. To investigate whether the secondary chemistry described above can affect the ratios of detected products, we have therefore performed kinetic modeling calculations using standard software.[24] Table 2 shows the reactions included in the kinetic model. We assumed our postulated branching ratios of $\phi_{1a} = 0.63$ and $\phi_{1b} = 0.37$ and calculated yields of CO, CO_2, and NO. As expected, we find that predicted product yields are substantially greater when the OH + CH_2O reaction is included in the model, although the exact amounts are very sensitive to the details of the rate parameters used. The [CO]/([CO] + [CO_2]) ratio predicted by the model is always 0.63 ± 0.01, however, regardless of the presence of the OH + CH_2O or any of the other secondary chemistry, and [CO] production by secondary sources is predicted to be at least 2 orders of magnitude smaller than [CO] from the title reaction. We can therefore state with confidence that our branching ratio result is unaffected by the secondary chemistry present in our experiments.

Comparing our results with literature values, we obtain excellent agreement with the modeling study of He et al.[6] for the ratio of CO and CO_2 producing channels. Our CO_2 yield is somewhat lower than the results of Guo et al.,[7] but all the studies shown in Table 1 are in agreement that channel 1b rather than channel 1d is responsible for most of the observed CO_2. The primary point of disagreement between our results and previous studies is that we attribute the predominate CO formation channel to be (1a) rather than (1c). It is likely that formation of product channel 1a is not a concerted process, but

a sequential process in which CO + HONO products are initialy formed, and the HONO has sufficient internal energy to dissociate into OH + NO. It is therefore possible that excited HONO can be stabilized at sufficiently high pressures. This may partially account for the disagreement between studies, as our work was carried out at total pressures of 1.0−1.5 Torr, while the studies reported in refs 6 and 7 were at ∼48 and ∼6.5 Torr, respectively. Guo et al.[7] detected a very weak HONO absorption signal at 3590.41 cm^{-1} but were unable to obtain a number density because the absorption coefficient was unknown. Their observation of HONO is therefore not really in contradiction to our observations. On the basis of our observed NO yields, we believe that the HONO channel 1c is quite minor.

It is tempting to speculate on possible reaction mechanisms. Two intermediate complexes are possible in this system:[7,8] HCO attack on the nitrogen atom of NO_2, forms an N−C bonded $CH(O)NO_2$ complex, which can rearrange via H atom migration to an oxygen atom, and dissociate to HONO + CO which can further fragment to OH + NO + CO. Alternatively, HCO attack on an oxygen atom of NO_2 forms and CH(O)ONO complex, which can dissociate to HCO_2 + NO → H + CO_2 + NO or undergo an H atom migration to the nitrogen atom, and dissociate to HNO + CO_2. Rearrangement between the two intermediate complexes involves a three-center C−N−O transition state and is probably unlikely. Of the two dissociation pathways for the CH(O)ONO complex, the first (via HCO_2) appears more likely, although it is conceivable that HNO formed by the second pathway could further fragment into the observed H + NO + CO_2 products. High-level ab initio calculations involving more detailed characterization of transition states of this system are clearly desirable.

Conclusion

Infrared diode laser spectroscopy was used to detect CO, NO, and CO_2 products in the HCO + NO_2 reaction at 298 K. By careful choice of photolytic precursor and reaction conditions, we have minimized secondary chemistry in this system and are therefore able to obtain branching ratios from product yield data in a direct manner. We find that the OH + NO + CO channel dominates this reaction, with a branching ratio of 0.63. The H + NO + CO_2 channel accounts for the remaining 37% of the reaction.

Acknowledgment. This work was supported by the Division of Chemical Sciences, Office of Basic Energy Sciences of the Department of Energy, Grant DE-FG03-96ER14645.

References and Notes

(1) Miller, J. A.; Bowman, C. T. *Prog. Energy Combust. Sci.* **1989**, *15*, 287.
(2) Chase, M. W., Jr.; et al. *J. Phys. Chem. Ref. Data* **1985**, *14* (Suppl. 1).
(3) Morrison, B. M., Jr.; Heicklen, J. *J. Photochem.* **1980,** *13*, 189.
(4) Morrison, B. M., Jr.; Heicklen, J. *J. Photochem.* **1981**, *15*, 131.
(5) Timonen, R. S.; Ratajczak, E.; Gutman, D. *J. Phys. Chem.* **1988**, *92*, 651.
(6) He, Y.; Kolby, E.; Shumaker, P.; Lin, M. C. *Int. J. Chem. Kinet.* **1989**, *21*, 1015.
(7) Guo, Y.; Smith, S. C.; Moore, C. B.; Melius, C. F. *J. Phys. Chem.* **1995**, *99*, 7473.
(8) Melius, C. F. In *Chemistry and Physics of Energetic Materials*; Bulusu, S. N., Ed.; Kluwer Academic Publishers: Dordrecht, The Netherlands, 1990; p 21.
(9) Atkinson, R.; Baulch, D. L.; Cox, R. A.; Hampson, R. F., Jr.; Kerr, J. A.; Troe, J. *J. Phys. Chem. Ref. Data* **1989**, *18*, 881.
(10) DeMore, W. B.; Sander, S. P.; Golden, D. M.; Hampson, R. F.; Kurylo, M. J.; Howard, C. F.; Ravishankara, A. R.; Kolb, C. E.; Molina, M. J. *Chemical Kinetics and Photochemical Data for Use in Stratospheric Modeling*, Evaluation #10, NASA/JPL Publication 92-20, 1992.
(11) Cooper, W. F.; Park, J.; Hershberger, J. F. *J. Phys. Chem.* **1993**, *97*, 3283.
(12) Lambrecht, R.; Hershberger, J. F. *J. Phys. Chem.* **1994**, *98*, 8406.
(13) Quandt, R. W.; Hershberger, J. F. *J. Phys. Chem.* **1996**, *100*, 9407.
(14) Taylor, H. A.; Denslow, R. R. *J. Phys. Chem.* **1927**, *31*, 374.
(15) Rothman, L. S.; et al. *J. Quant. Spectrosc. Radiat. Transfer* **1992**, *48*, 469.
(16) Okabe, H. *Photochemistry of Small Molecules*; Wiley: New York, 1978.
(17) Steiner, D. A.; Polo, S. R.; McCubbin, T. K., Jr.; Wishah, K. A. *J. Mol. Spectrosc.* **1983**, *98*, 453.
(18) Ferretti, E. L.; Rao, K. N. *J. Mol. Spectrosc.* **1974**, *51*, 97.
(19) Tsang, W.; Herron, J. T. *J. Phys. Chem. Ref. Data* **1991**, *20*, 609.
(20) Streit, G. E.; Wells, J. S.; Fehsenfeld, F. C.; Howard, C. J. *J. Chem. Phys.* **1978**, *70*, 3439.
(21) Baulch, D. L.; Cobos, C. J.; Cox, R. A.; Esser, C.; Frank, P.; Just, Th.; Kerr, J. A.; Pilling, M. J.; Troe, J.; Walker, R. W.; Warnatz, J. *J. Phys. Chem. Ref. Data* **1992**, *21*, 411.
(22) Atkinson, R.; Baulch, D. L.; Cox, R. A.; Hampson, R. F., Jr.; Kerr, J. A.; Troe, J. *J. Phys. Chem. Ref. Data* **1992**, *21*, 1125.
(23) Kita, D.; Stedman, D. H. *J. Chem. Soc., Faraday Trans. 2* **1982**, *78*, 1249.
(24) Braun, W.; Herron, J. T.; Kahaner, D. *Int. J. Chem. Kinet.* **1988**, *20*, 51.